



MDCA – MAIAC Desert Calibration Algorithm (MODIS, VIIRS, commercial satellite data)

MAIAC: A. Lyapustin, Y. Wang, M. Choi

with contributions from

MCST/VCST: X. Xiong, A. Angal, A. Wu

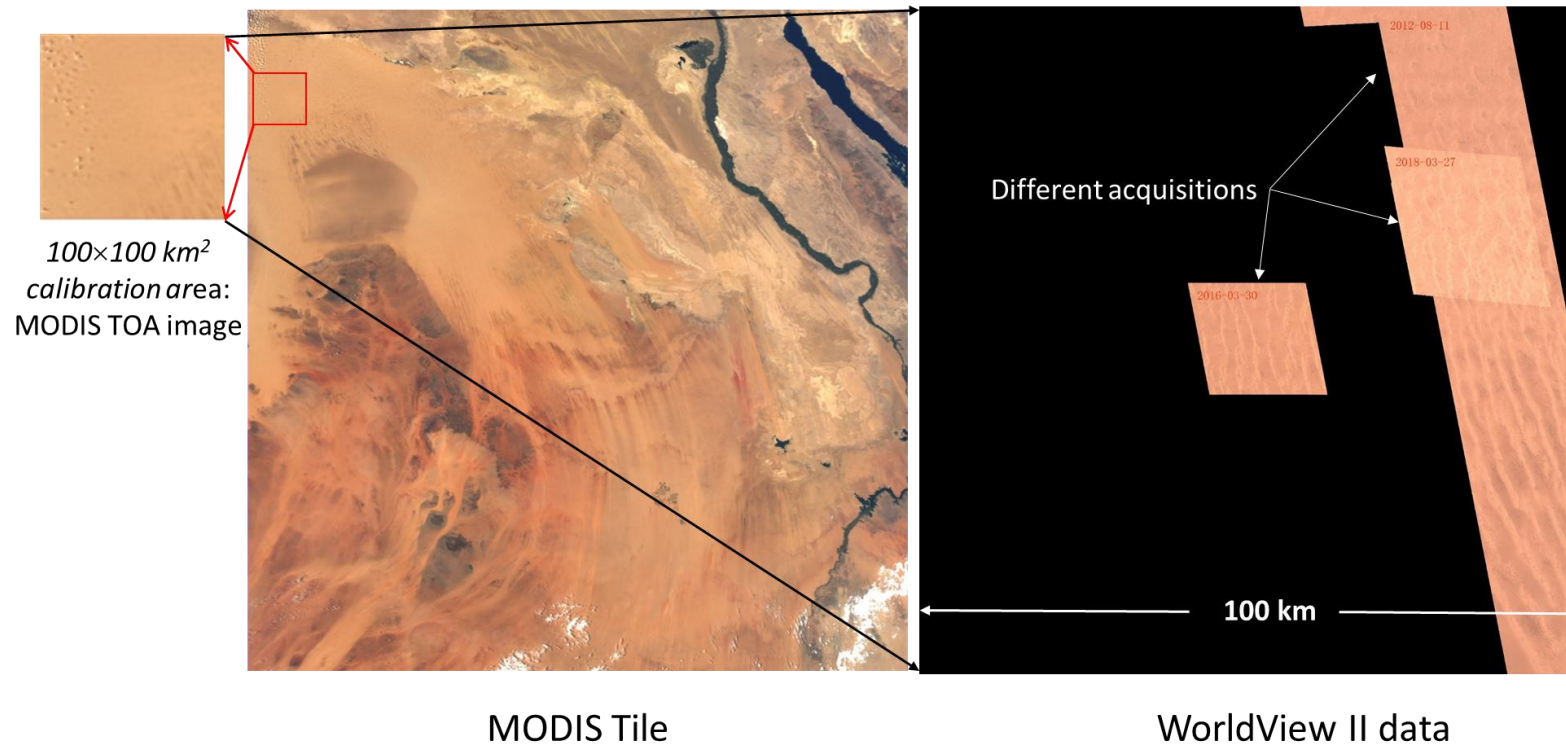
LaRC: D. R. Doelling, R. Bhatt

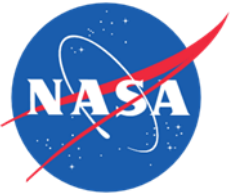


MDCA Introduction

- MDCA relies on **global daily** Earth Science Data products from the Multi-Angle Implementation of Atmospheric Correction (MAIAC) algorithm ([Lyapustin et al., AMT, 2018](#)).
- MAIAC reports **CM, AOD, CWV, spectral BRDF**, etc. from MODIS T&A (1 km), VIIRS SNPP, J1, J2 (0.75 km).
- MDCA uses observations over Libya-4 CEOS site.

Example of WV2 Data Over Libya-4 Site





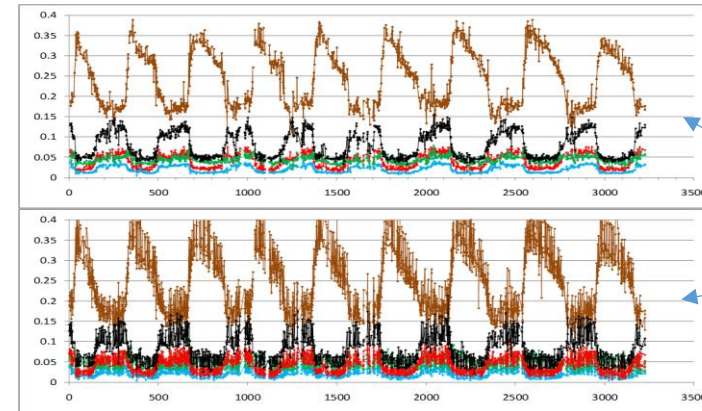
MDCA Main Steps: Example for MODIS C5

Method:

- 1) Perform MAIAC retrievals (CM, AOT, WV, BRDF etc.);
- 2) Compute TOA reflectance (R_n) for a fixed view geometry ($VZA=0^\circ$, $SZA=30^\circ$) and evaluate trends in both Terra and Aqua;
- 3) Apply de-trending and compute Terra-Aqua X-calibration factor (gain correction for Terra)

(Lyapustin et al., AMT, 2014)

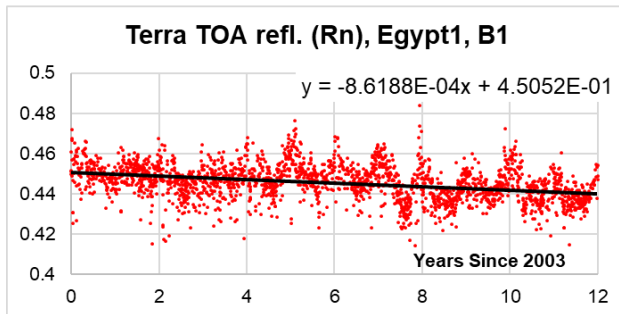
Lyapustin et al., 2012, RSE



BRDF normalization reduces variability by a factor of ~3-5!

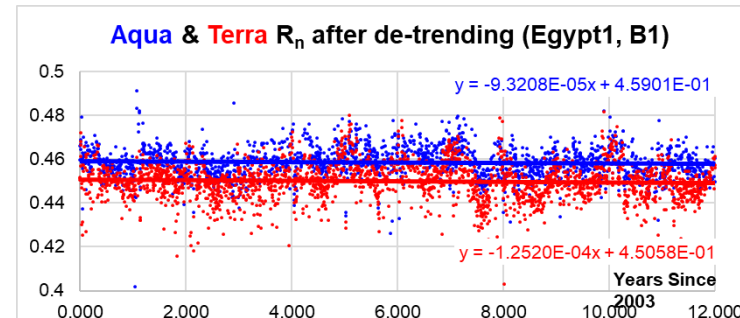
Normalized BRF_n

Original BRF (Red, Green, Blue, NIR, SWIR)



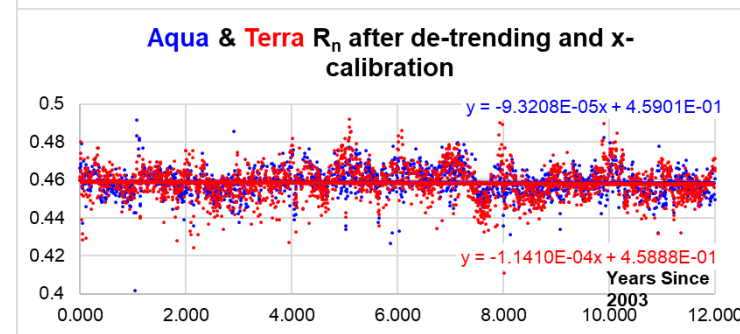
Average trend/year/unit_refl.

	Δ_{Terra}	σ_{Terra}	Δ_{Aqua}	σ_{Aqua}
TOA_B01	-1.6884E-03	2.6114E-04	1.5848E-06	3.9377E-04
TOA_B02	7.7780E-04	2.4303E-04	-6.5120E-05	3.5583E-04
TOA_B03	-8.8922E-04	4.5314E-04	-3.1763E-04	2.8486E-04
TOA_B04	-5.6629E-04	3.2829E-04	-3.9831E-05	5.0202E-04
TOA_B05	1.9477E-04	3.3019E-04	4.5784E-06	3.3528E-04
TOA_B06	-3.9516E-04	3.0211E-04	-3.1194E-04	2.8191E-04
TOA_B07	2.0259E-04	2.4491E-04	-5.8419E-04	3.2705E-04
TOA_B08	-1.2627E-03	1.0018E-03	-5.5178E-04	1.0915E-04
TOA_B09	-3.9874E-04	5.2176E-04	1.3724E-04	2.1120E-04
TOA_B10	-7.2800E-04	8.2601E-04	-3.0632E-04	7.1498E-04



Average X-gain for Terra

	Average	Stdev
TOA_B01	1.018776	0.000949
TOA_B02	1.000523	0.001054
TOA_B03	0.989436	0.001268
TOA_B04	1.00109	0.001448
TOA_B05	0.98862	0.001855
TOA_B06	0.997128	0.000898
TOA_B07	0.999368	0.000373
TOA_B08	1.003774	0.000948
TOA_B09	1.0014	0.001488
TOA_B10	1.014141	0.002077



Developed calibration became a standard part of MODIS Land Discipline Processing in Collections C6 and C6.1.



MDCA - SNO Comparison for MODIS C7

SNO data: courtesy of D. Doelling

MODIS band	SNO Terra/Aqua scaling	SNO Stderr (%)	SNO T/A Trend %/20yr	MAIAC Terra/Aqua scaling	MAIAC/SNO	MAIAC T/A trend %/20yr
0.65 μ m	0.9961	0.13	+0.048	1.0013	+0.52	-0.016
0.86 μ m	0.9903	0.23	+0.314	0.9961	+0.59	+0.006
0.47 μ m	0.9861	0.22	-0.398	0.9882	+0.21	+0.01
0.55 μ m	1.0013	0.15	+0.186	1.0003	-0.10	-0.25
1.24 μ m	0.9783	0.35	+0.66	0.9929	+1.50	-0.68
1.64 μ m	0.9887	0.42	+0.148	0.9982	+1.16	-0.42
2.13 μ m	1.0061	0.35	-0.148	1.0006	-0.67	-0.532
1.37 μ m	1.0754	0.99	+2.632			



MDCA Analysis of VIIRS

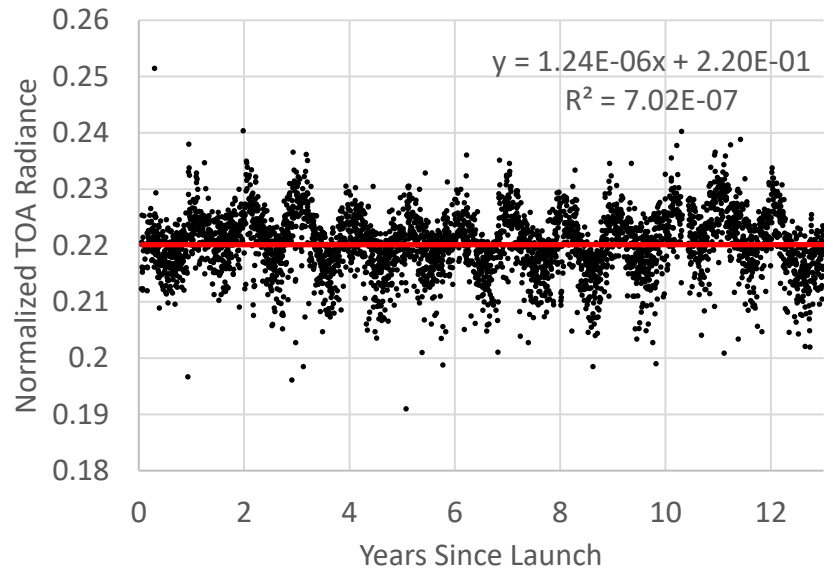
Use the latest versions of L1B data:

- MODIS C6.1 with polarization correction, de-trending and Terra-to-Aqua cross-calibration;
- VIIRS SNPP C2.0
- VIIRS JPSS1 C2.1
- VIIRS JPSS2



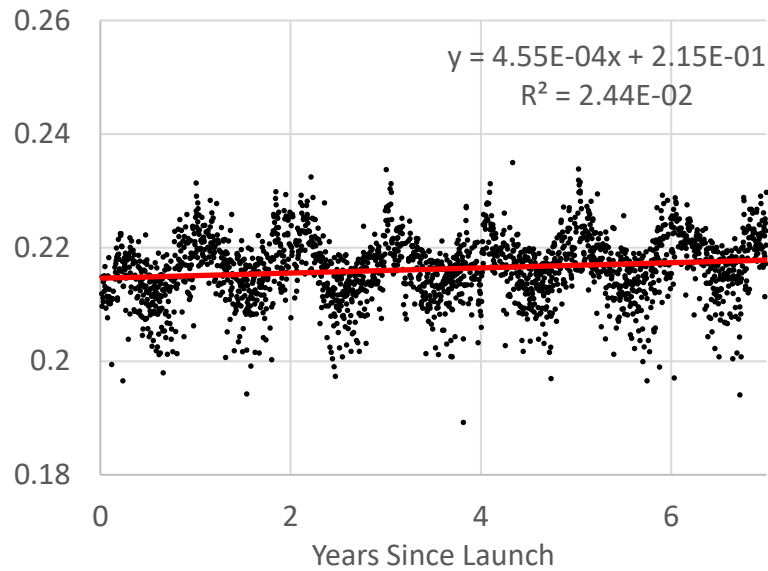
VIIRS SNPP/J1/J2 Normalized TOA Reflectance Time Series (Blue Band)

B8(M1)



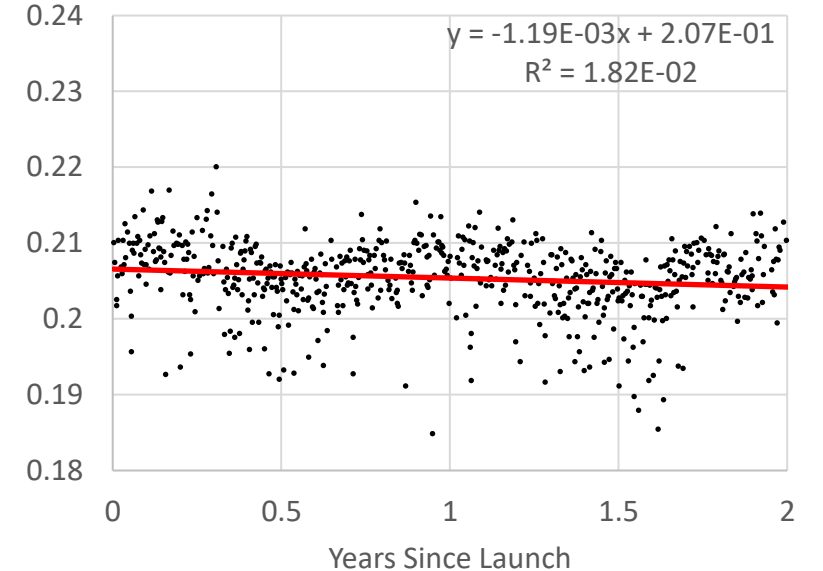
SNPP

B8(M1)



NOAA-20

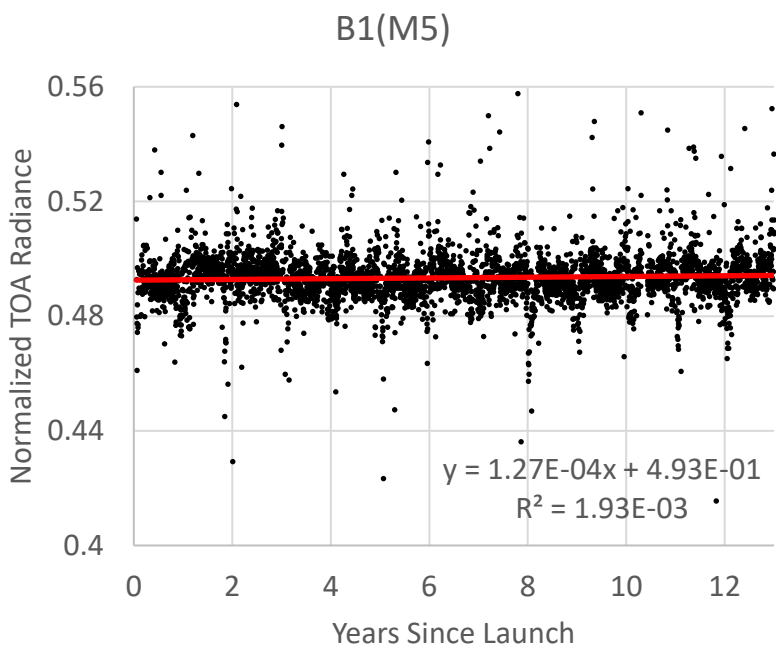
B8(M1)



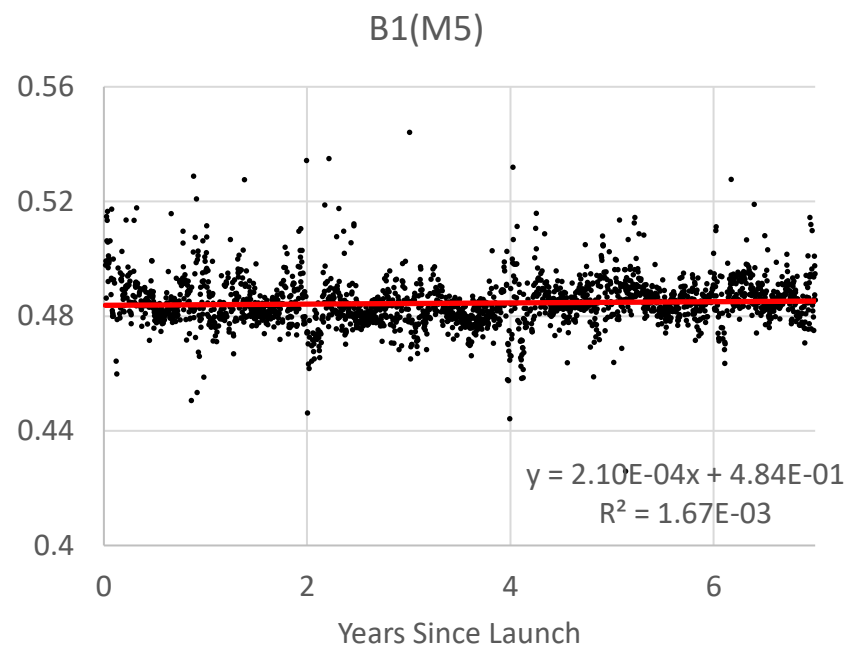
NOAA-21



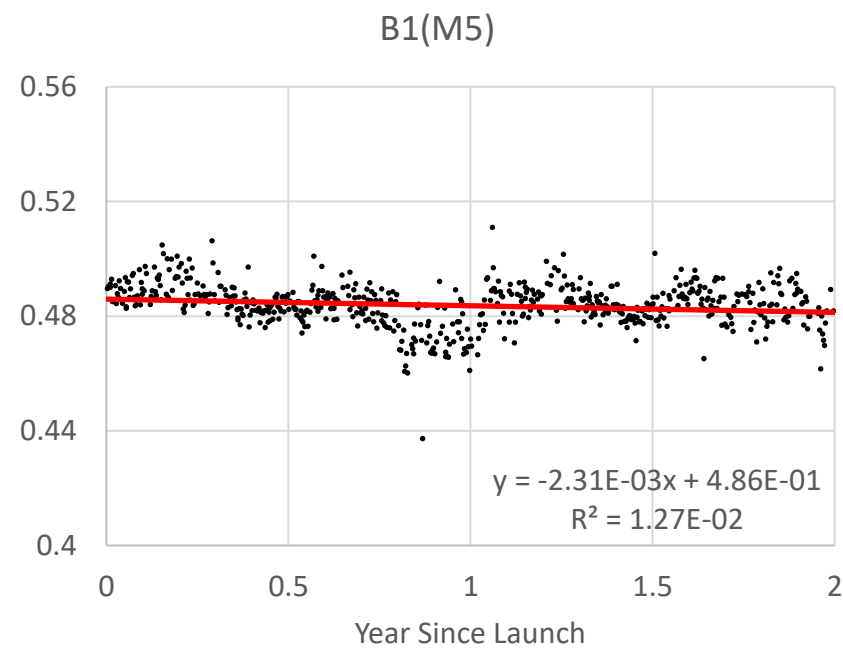
VIIRS SNPP/J1/J2 Normalized TOA Reflectance Time Series (Red Band)



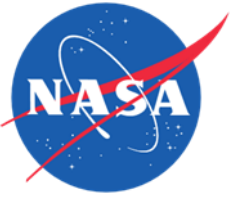
SNPP



NOAA-20



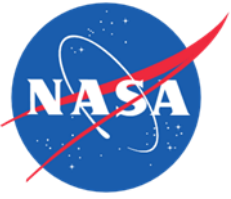
NOAA-21



VIIRS Calibration Trends

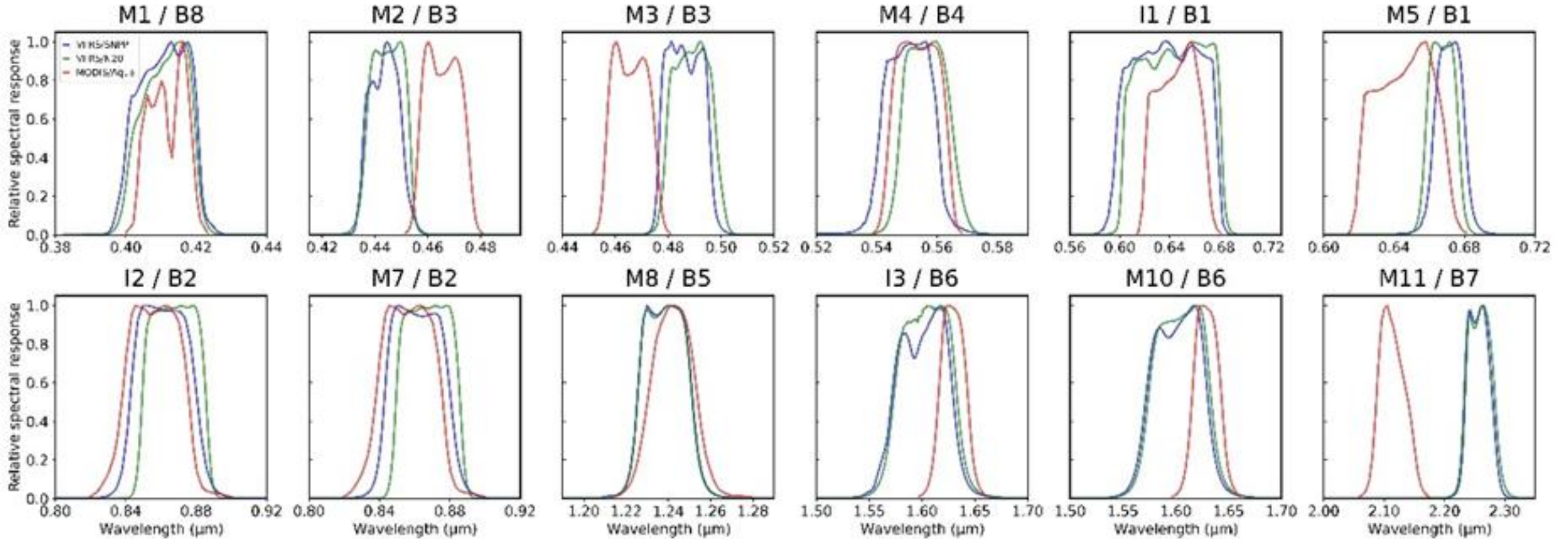
Band	Intercept			Slope			Slope/Intercept (Trend/year/unit of refl.)		
	SNPP	N20	N21	SNPP ($\times 10^{-3}$)	N20 ($\times 10^{-3}$)	N21($\times 10^{-3}$)	SNPP	N20	N21
M1	0.224	0.209	0.207	-0.016 ± 0.027	$-1.12 \pm 0.16/-0.8$	-1.19 ± 0.35	$-7.16E-05$	$-5.35E-03$	$-5.74E-03$
M2	0.230	0.219	0.218	-0.13 ± 0.033	$-0.98 \pm 0.15/-1.3$	-1.74 ± 0.34	$-5.55E-4$	$-4.47E-03$	$-7.97E-03$
M3	0.251	0.240	0.240	-0.055 ± 0.027	$-0.98 \pm 0.12/-2$	-1.69 ± 0.39	$-2.20E-04$	$-4.08E-03$	$-7.05E-03$
M4	0.340	0.336	0.336	-0.063 ± 0.029	$-1.24 \pm 0.15/-1.4$	-2.99 ± 0.58	$-1.84E-04$	$-3.67E-03$	$-8.90E-03$
M5	0.499	0.476	0.490	-0.073 ± 0.034	$-0.53 \pm 0.17/-0.7$	-2.31 ± 0.82	$-1.47E-04$	$-1.11E-03$	$-4.76E-03$
M7	0.586	0.565	0.562	-0.31 ± 0.043	$-0.26 \pm 0.22/-0.8$	-1.51 ± 0.95	$-5.31E-04$	$-4.64E-04$	$-2.68E-03$
M8	0.662	0.645	0.634	-0.44 ± 0.052	$-0.11 \pm 0.28/0.9$	-0.69 ± 1.04	$-6.57E-04$	$-1.74E-04$	$-1.07E-03$
M10	0.696	0.681	0.660	-0.39 ± 0.046	$0.81 \pm 0.29/0.0$	-1.28 ± 1.14	$-5.61E-04$	$1.19E-03$	$-1.94E-03$
M11	0.587	0.576	0.577	-0.59 ± 0.063	-1.49 ± 0.35	-3.45 ± 1.22	$-1.00E-03$	$-2.59E-03$	$-5.98E-03$
I1	0.463	0.451	0.458	-0.31 ± 0.071	$-0.82 \pm 0.28/-1.5$	-1.49 ± 0.90	$-6.70E-04$	$-1.83E-03$	$-3.25E-03$
I2	0.585	0.563	0.573	-0.37 ± 0.070	$0.004 \pm 0.26/-0.5$	-0.67 ± 0.82	$-6.28E-04$	$7.03E-06$	$-1.16E-03$
I3	0.706	0.670	0.714	-0.59 ± 0.085	$0.71 \pm 0.30/\sim 0.0$	-4.50 ± 1.21	$-8.43E-04$	$1.07E-03$	$-6.29E-03$

Table 1. Results from trend analysis of SNPP, N20, N21 VIIRS including slope and intercept of linear regression, and ratio slope/Intercept in units of reflectance (change)/unit reflectance/year. For N20, a second value separated by ‘/’ gives the VCST trend (Twedt et al., 2022).



VIIRS X-Cal to MODIS Aqua

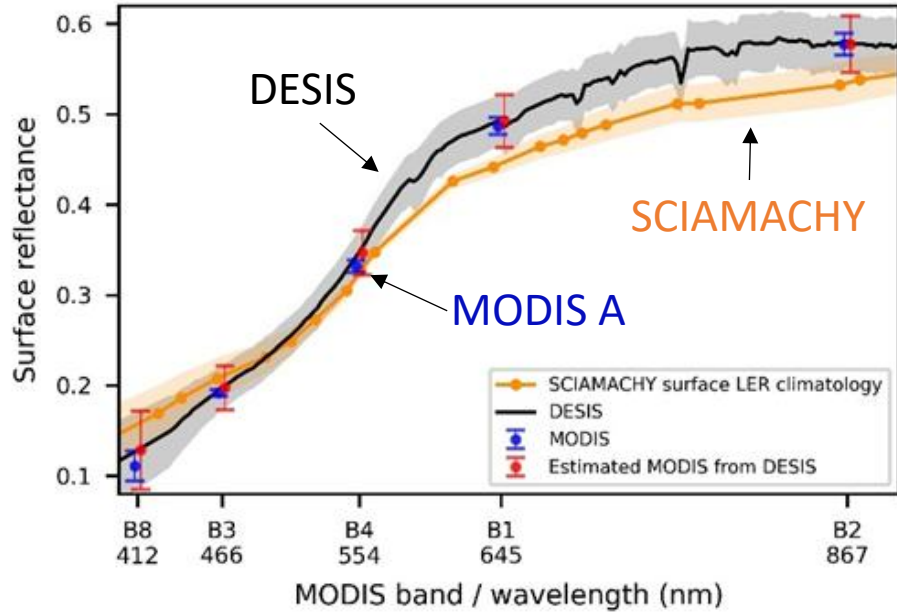
Because bands are different, sensors measure different reflectance over the same targets (with spectral dependence), we need to account for the RSR differences





Spectral Band Adjustment Factor (SBAF)

- DESIS - DLR Earth Sensing Imaging Spectrometer, on ISS since 2018 (400-1000nm, spectral sampling at 2.55 nm and res. of 3.5 nm; 30m spatial resolution and ~ 30km swath). By our request, 97 DESIS measurement granules were collected over Libya-4 during 2018–2021. 12 are good.



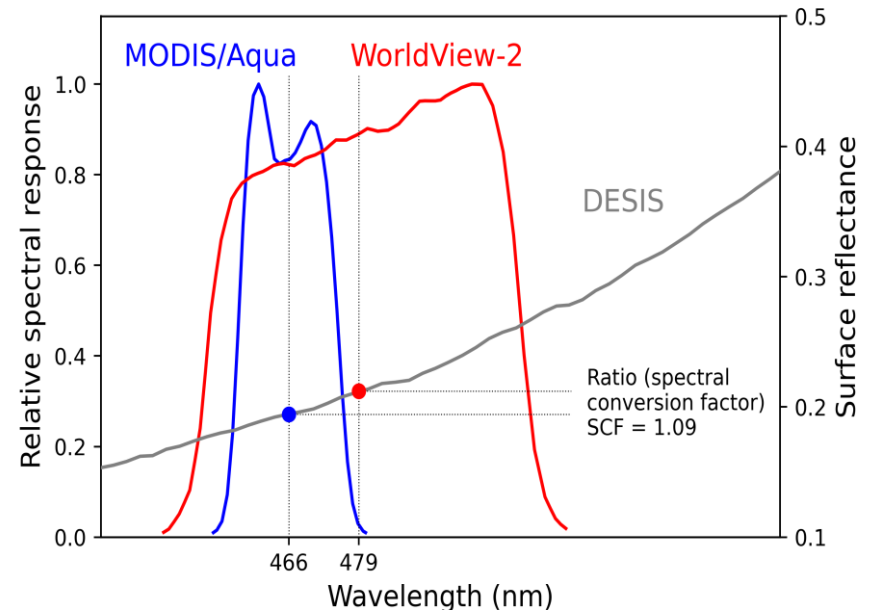
SBAF is generated for:

5×5 M-pixels,
10×10 I-pixels
~4×4km² area

- Spectral convolution of surface reflectance

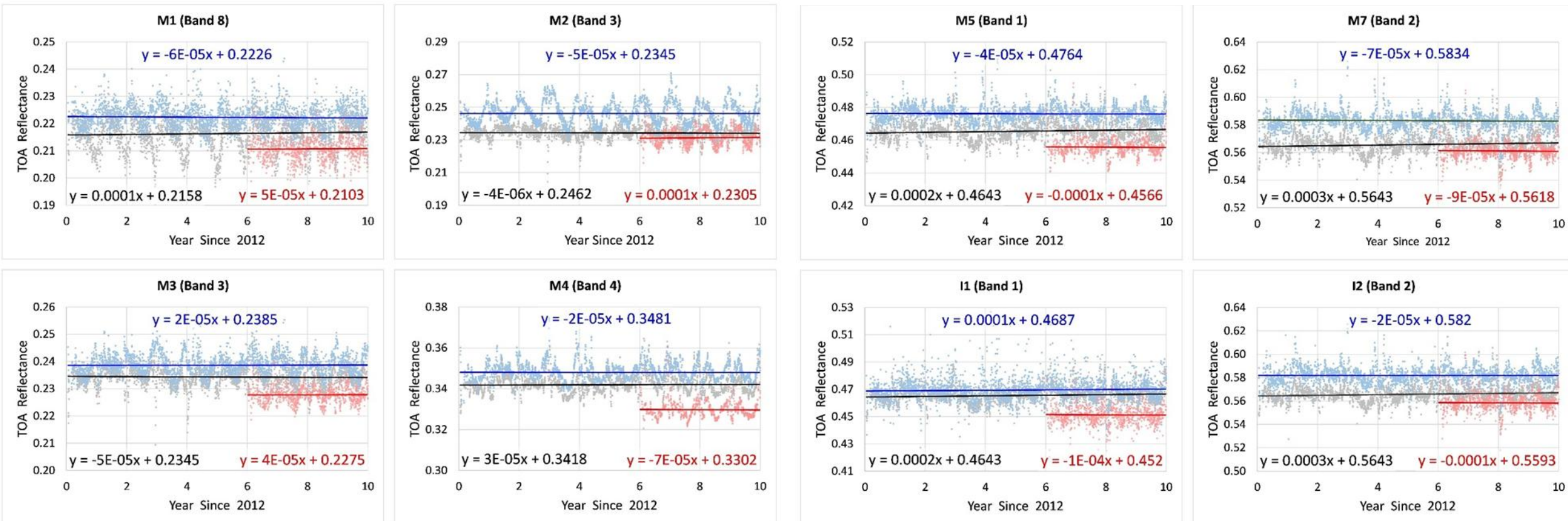
$$\rho_{simulated} = \frac{\sum \rho_{\lambda} RSR_{\lambda} d\lambda}{\sum RSR_{\lambda} d\lambda}$$

- ρ_{λ} : DESIS surface reflectance with high spectral resolution
- RSR_{λ} : spectral response function

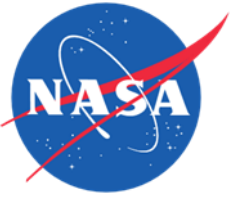




VIIRS X-Calibration to MODIS Aqua



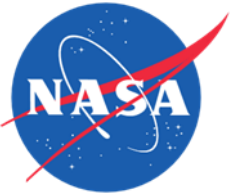
VIIRS BRDF is multiplied by the SBAF (this effectively “shifts” the VIIRS band to the MODIS reference band), and VIIRS normalized TOA reflectance is computed at the MODIS wavelength. This way, both surface and atmospheric RT computations are done at the same wavelength ensuring 1:1 comparison.



Aqua/VIIRS SNPP/J1/J2 X-calibration Summary

Band	SBAF		X-calibration Coefficients			
	Aqua/SNPP	Aqua/J1	Aqua/SNPP	Aqua/J1	SNPP/J1	J1/J2
B8/M1	0.960	1.001	0.974 ± 0.033	1.028 ± 0.034	1.055 ± 0.028	1.039±0.038
B3/M2	1.197	1.191	0.952 ± 0.031	1.014 ± 0.026	1.065 ± 0.034	1.009±0.034
B3/M3	0.889	0.882	0.982 ± 0.023	1.029 ± 0.021	1.048 ± 0.021	1.022±0.033
B4/M4	1.026	0.978	0.983 ± 0.018	1.037 ± 0.018	1.055 ± 0.018	1.023±0.036
B1/M5	0.959	0.962	0.978 ± 0.017	1.021 ± 0.017	1.044 ± 0.016	0.996±0.032
B2/M7	1.001	0.999	0.971 ± 0.017	1.008 ± 0.017	1.039 ± 0.017	1.004±0.032
M8	-	-	-	-	1.026 ± 0.017	1.017±0.033
M10	-	-	-	-	1.022 ± 0.016	1.042±0.035
M11	-	-	-	-	1.020 ± 0.040	1.001±0.042
B1/I1	1.016	1.004	0.992 ± 0.023	1.032 ± 0.021	1.040 ± 0.026	1.013±0.040
B2/I2	1.001	0.998	0.973 ± 0.018	1.013 ± 0.018	1.042 ± 0.019	1.003±0.028
I3	-	-	-	-	1.054 ± 0.018	1.003±0.035

Table 2. Spectral Band Adjustment Factor (SBAF) for SNPP and J1 VIIRS to MODIS Aqua, and pair-wise cross-calibration coefficients among the three sensors.



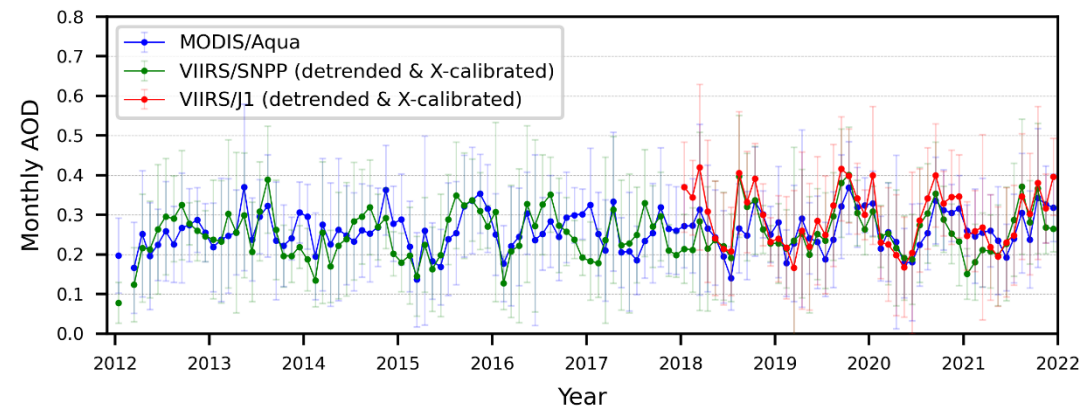
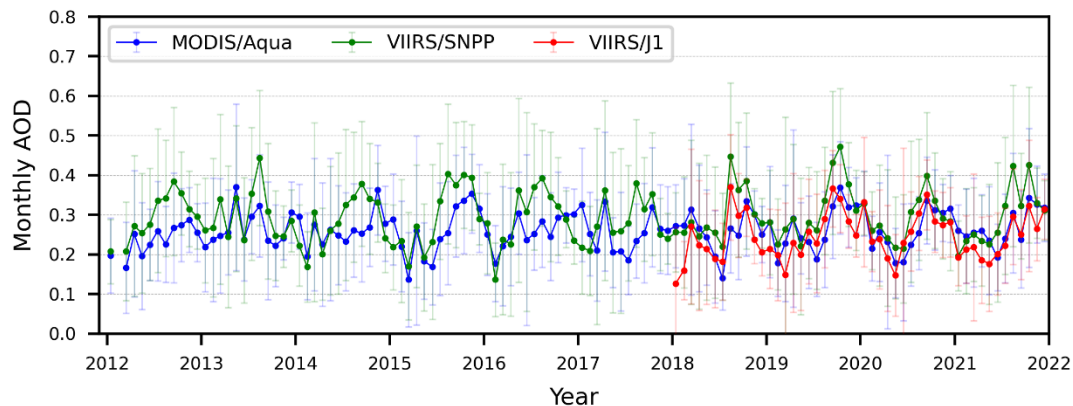
VIIRS SNPP/J1/J2 X-calibration Summary

Band	SNPP/JPSS1			JPSS1/JPSS2	
	MDCA	VCST (2025)	LaRC (2022)	MDCA	VCST (2025)
M1 (0.41)	5.5	6.4-7.7	-	3.9	-0.2 to +1.8 (3.7 DomeC)
M2 (0.45)	6.5	5.3-6.2	-	0.9	0.4, 0.8 (L4, DCC); 2.3, 4.1 (SNO, DomeC)
M3 (0.49)	4.8	3.8-5.6	5.6±0.2	2.2	0.4-1.4 (1.9 SNO)
M4 (0.56)	5.5	3.1-4.7 (6.8 DCC)	5.8±0.2	2.3	-1.7 to 1.3
M5 (0.67)	4.4	4.3-5.0	5.4±0.2	-0.4	-0.4,-0.5 (SNO, L4), -1.3, 0.6 (DCC, DomeC)
M7 (0.87)	3.8	2.0-2.8 (4.8 DCC)	4.2±0.2	0.4	0.4,0.5 (L4, DCC), -1.1, 1.1 (DomeC, SNO)
M8 (1.24)	2.6	1.8-3.0	2.0±0.2	1.7	0.8-3.0
M10 (1.66)	2.2	1.8-2.9 (0.3 DCC)	2.5±0.3	4.2	2.2-2.9 (3.9 L4)
M11 (2.25)	2.0	1.5-1.9	1.6±0.5	0.1	-0.3 (DCC), 1.6 (L4)
I1 (0.64)	4.0	2.3-2.8 (4.4 DCC)	4.8±0.2	1.3	-0.7 to 0.6 (1.3 DCC)
I2 (0.87)	4.2	2.3-2.6 (5.4 DCC)	-	0.3	0.1 (L4, DCC), -1.2 to 11 (DomeC, SNO)
I3 (1.61)	5.4	2.5-3.8	5.0±0.3	0.3	-0.3 (DCC), 2.3 (SNO, L4)

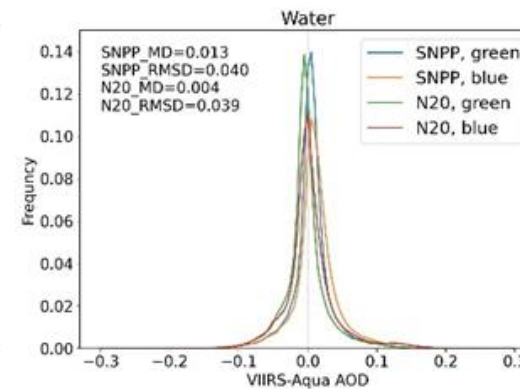
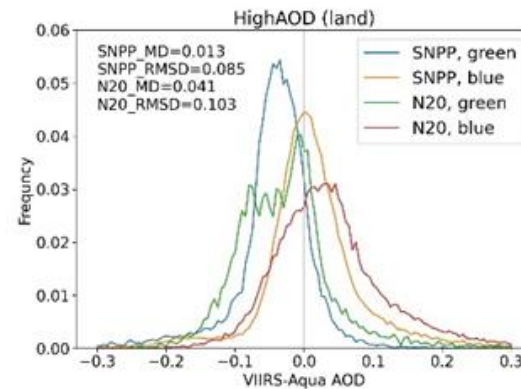
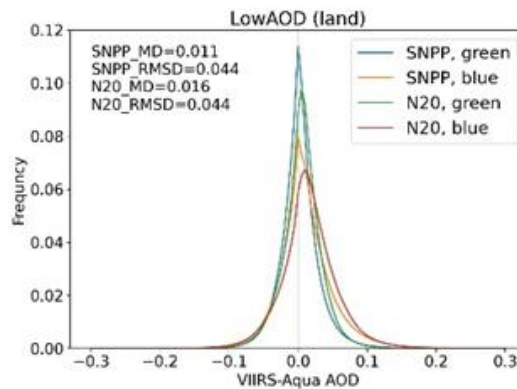
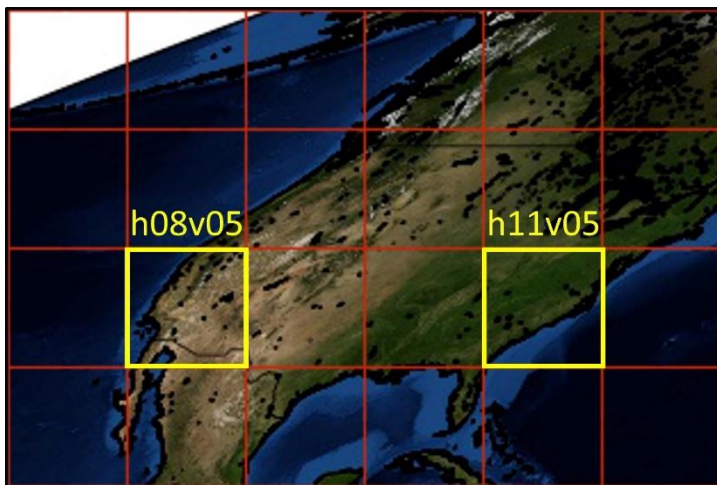
Table 3. Cross-calibration biases (%) among VIIRS SNPP (S) and VIIRS J1, J2 from different sources. VCST – Libya-4, Dome C, Aqua SNO, DCC (A. Wu et al., 2025); LaRC - Desert, Dome C, Ray Matching, DCC.



MAIAC MODIS-VIIRS Continuity Analysis



AOD over Libya-4 Before and After X-Calibration

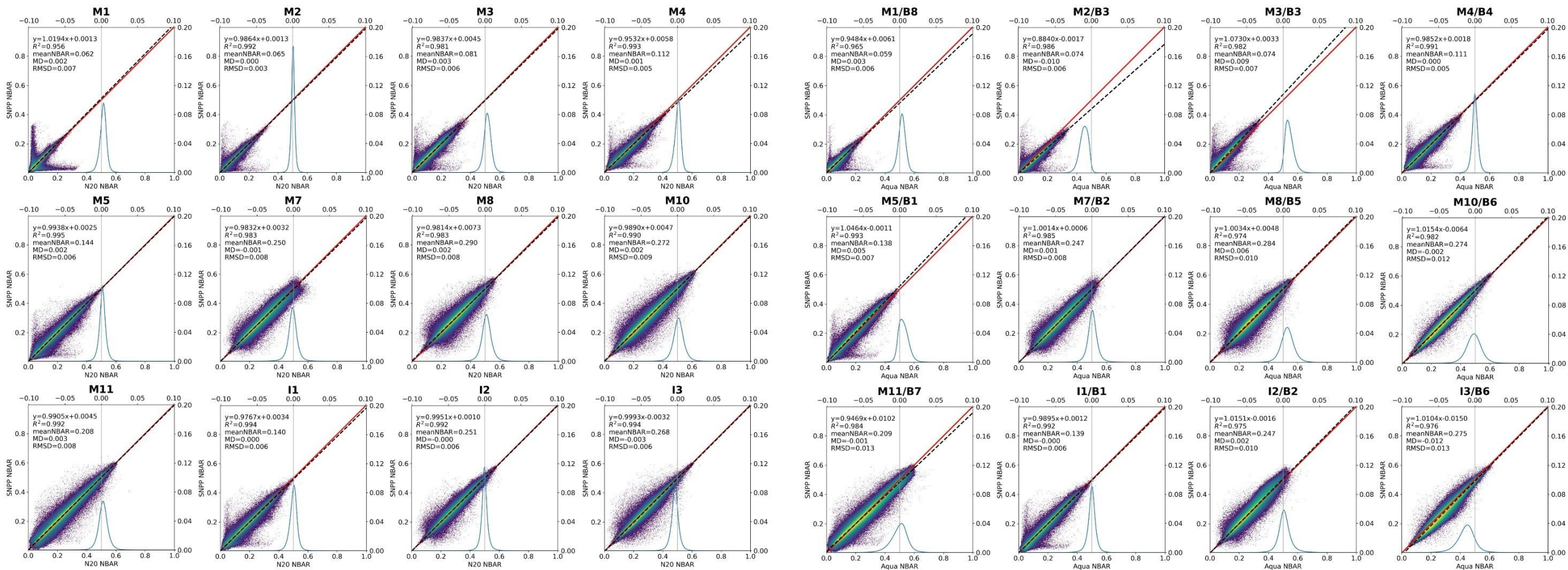


2 tiles, 4 years of data (2018-2021)



Spectral NBAR Comparison

NBAR – nadir BRDF-adjusted reflectance (nadir + local sun at 1:30pm)



SNPP vs NOAA 20

SNPP vs Aqua

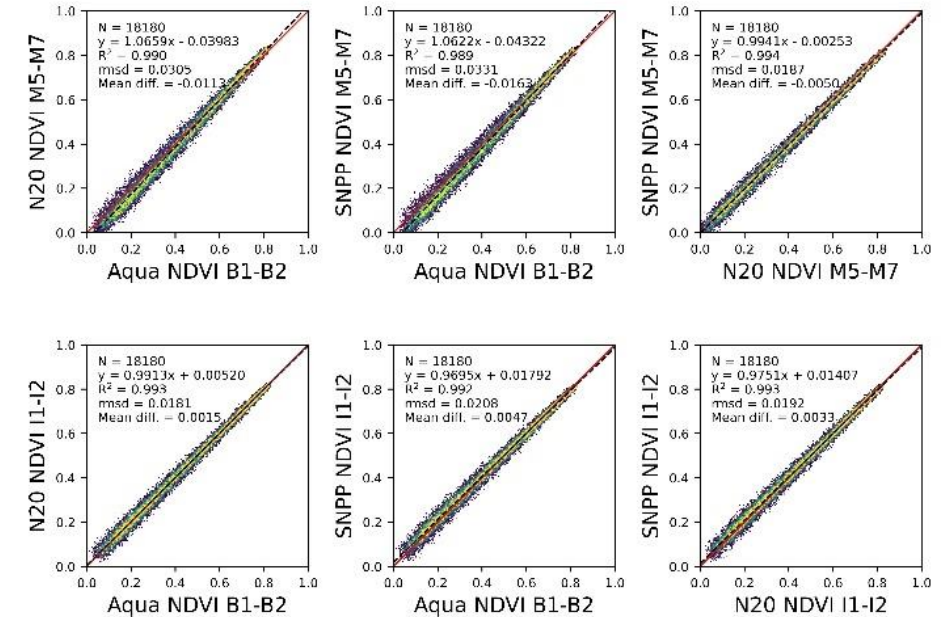
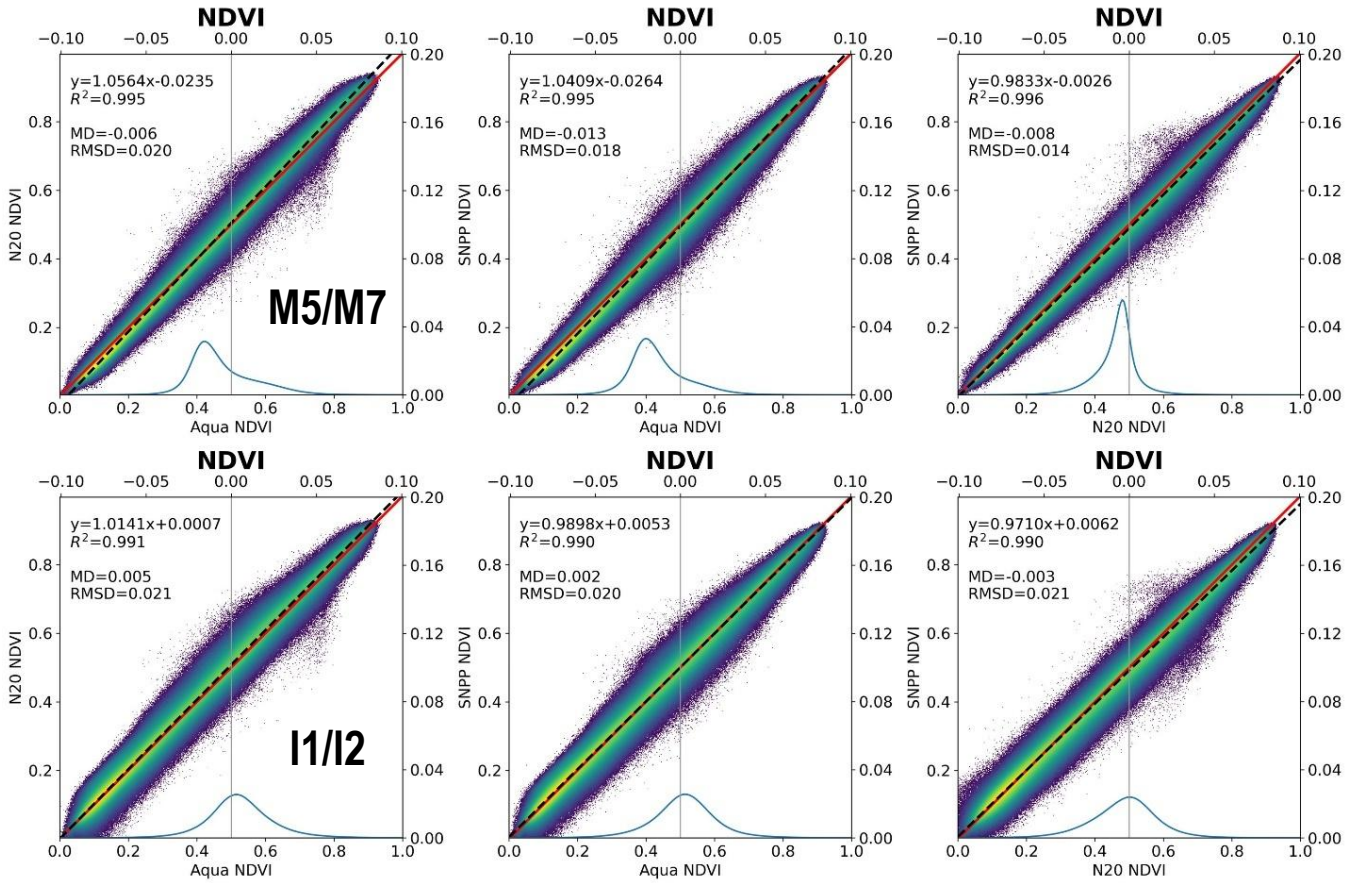
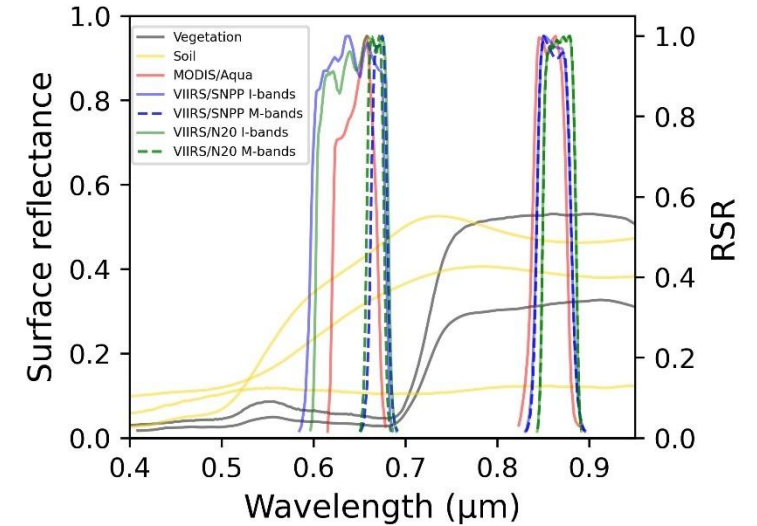
RMSD of 0.005-0.007 in the darker visible and of 0.008-0.013 in brighter NIR-SWIR bands



NDVI Analysis

Center Wavelength (nm)

	SNPP (M/I)	N20	A
Red	671/638	668/643	646
NIR	861/861	868/867	856

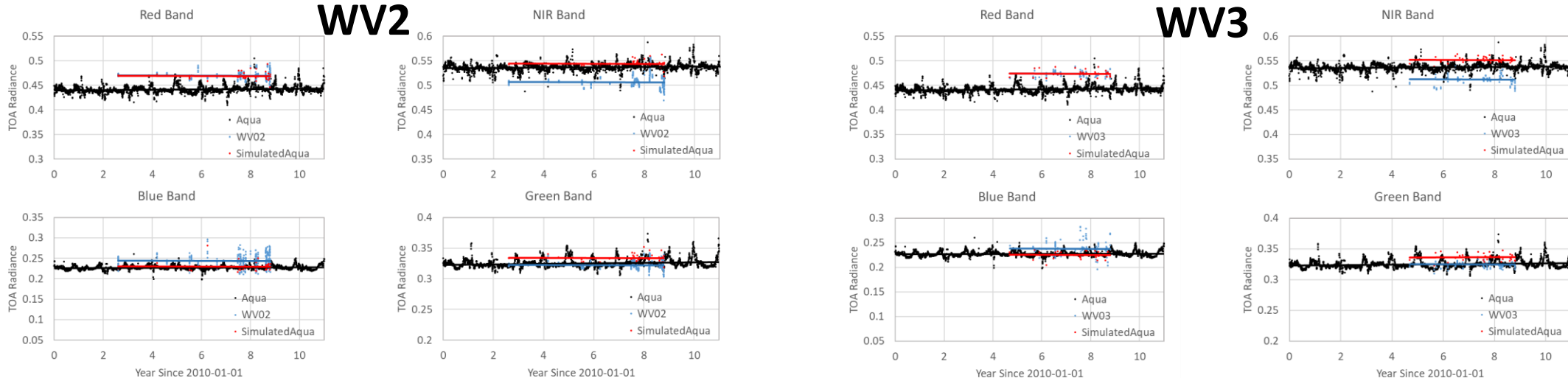


The MODIS – VIIRS NDVIs agree within $rmsd \sim 0.02$ and an average MD -0.01 for $NDVI_M$ and 0.003 for $NDVI_I$.



Example: MDCA Analysis of DG

Applied to: Satellogic (Newsat-10/27/31/41), Airbus Pleiades (PHR1A, PHR1B), Pleiades Neo (PNEO3, PNEO4), SPOT (SPOT6), Maxar (now Vantor) Legion (LG-1 to 4)



X-cal Factors (DG/Aqua)

Band	GeoEye	QuickBird	WV02	WV03
Blue	1.0350	1.0194	1.0156	0.9956
Green	1.0290	1.1180	1.0343	1.0424
Red	1.0838	1.0959	1.0689	1.0799
NIR	1.0267	1.0670	1.0189	1.0321
N Samp	62	5	35	32

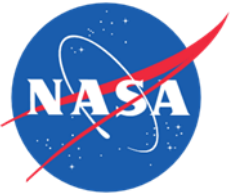
Summary

1. Results for QuickBird are not reliable (low stats)
2. DG sensors are within ~2-3% of each other
3. DG are systematically higher than Aqua:
 - Blue: 0-3.5% (0-1.6%)
 - Green: 2.9-4.2% (3.4-4.2%)
 - Red: 6.9-8.4% (6.9-8%)
 - NIR: 1.9-3.2% (1.9-3.2%)

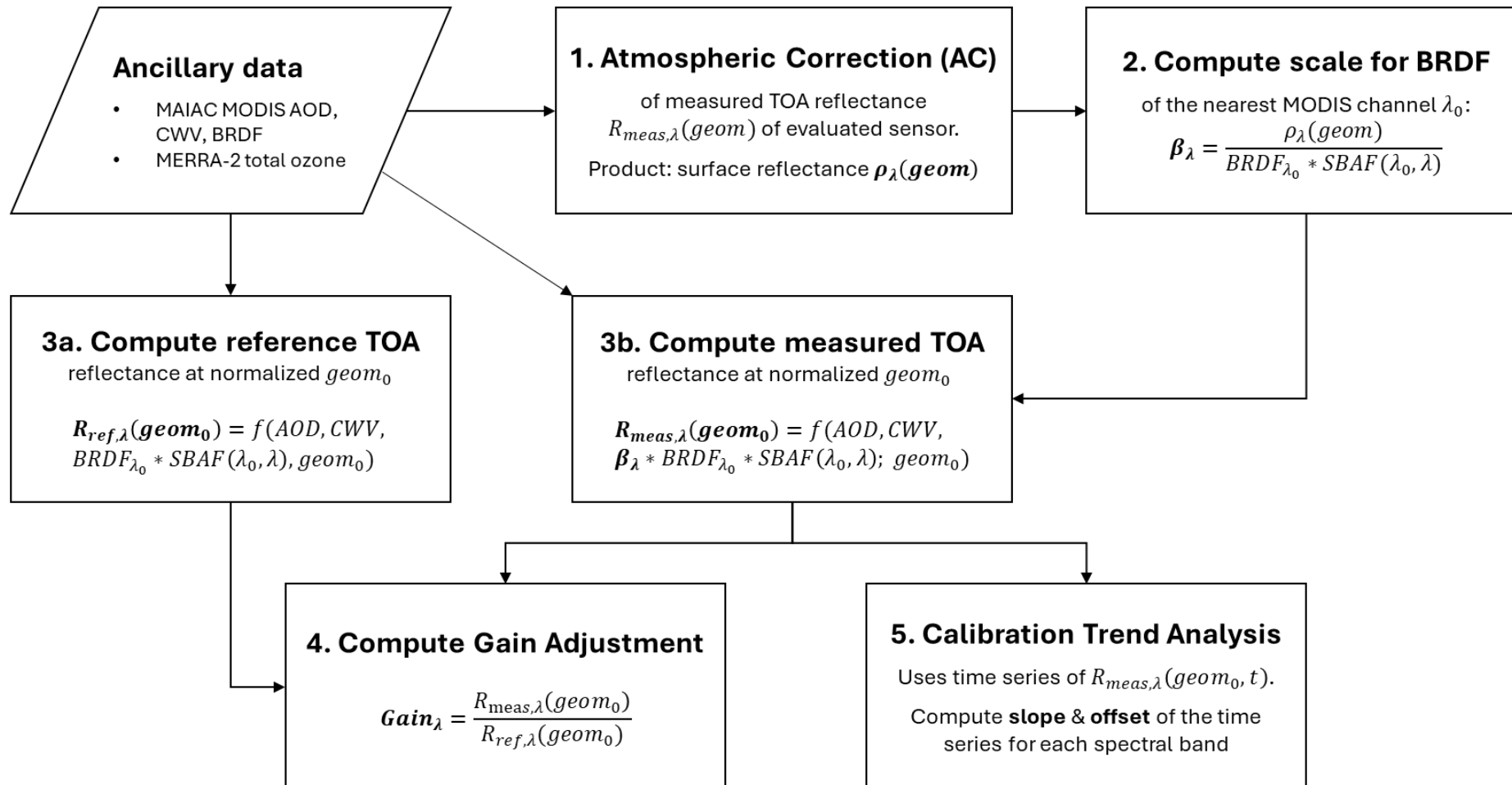
Lyapustin, A., Wang, Y., Xiong, X., Meister, G., Platnick, S., Levy, R., Franz, B., Korkin, S., Hilker, T., Tucker, J., Hall, F., Sellers, P., Wu, A., & Angal, A. (2014). Scientific impact of MODIS C5 calibration degradation and C6+ improvements. *Atmospheric Measurement Techniques*, 7(12), 4353–4365. <https://doi.org/10.5194/amt-7-4353-2014>

Lyapustin, A., Wang, Y., Choi, M., Xiong, X., Angal, A., Wu, A., Doelling, D. R., Bhatt, R., Go, S., Korkin, S., Franz, B., Meister, G., Sayer, A. M., Roman, M., Holz, R. E., Meyer, K., Gleason, J., & Levy, R. (2023). Calibration of the SNPP and NOAA 20 VIIRS sensors for continuity of the MODIS climate data records. *Remote Sensing of Environment*, 295, 113717. <https://doi.org/10.1016/j.rse.2023.113717>

Choi, M., Lyapustin, A., Wang, Y., Tucker, C. J., Khan, M. N., Policelli, F., Neigh, C. S. R., & Hall, A. A. (2024). Calibration of Maxar Constellation Over Libya-4 Site Using MAIAC Technique. *IEEE Journal of Selected Topics in Applied Earth Observations and Remote Sensing*, 17, 5460–5469. <https://doi.org/10.1109/JSTARS.2024.3367250>



Backup: MDCA Processing Diagram



λ = Bands of commercial satellites; λ_0 = nearest MODIS bands

$geom$ = view geometry of measurements; $geom_0$ = normalized view geometry

R_{meas} = TOA reflectance of commercial satellites; R_{ref} = TOA reflectance of reference MODIS

ρ_{λ} = Surface reflectance; $BRDF_{\lambda_0}$ = MAIAC BRDF at MODIS bands at $geom$

$SBAF$ = Spectral band adjustment factor of surface reflectance between λ and λ_0